Experimental study of H-L transitions in JET

C.F. Maggi[1], E. Delabie[2], N. Hawkes[3], M. Lehnen[4], G. Calabro'[5], F. Rimini[3], E.R. Solano[6] and JET EFDA Contributors[*]

JET-EFDA, Culham Science Centre, Abingdon, OX14 3DB, UK
[1]MPI für Plasmaphysik, EURATOM Association, 85748 Garching, Germany
[2]Association EURATOM-FOM, Nieuwegein, The Netherlands
[3]CCFE/Fusion Association, Culham Science Centre, Abingdon, OX14 3DB, UK
[4]ITER Organization, 13115 Saint Paul Lez Durance, France; [5]Associazione EURATOM-ENEA, Frascati, Italy; [6]Asociación EURATOM/CIEMAT, Madrid, Spain
** See App. of F. Romanelli et al., Proc. of the 24th IAEA Fusion Energy Conf., 2012, San Diego, USA*

1. Introduction. ITER operation scenarios foresee the access to H-mode with limited additional heating at low density, followed by an increase in density and power while remaining in H-mode to the required operating conditions [1]. Such scheme is thus sensitive to the level of hysteresis in the H-mode power and to the competing evolution of input power, density and radiation losses from the bulk plasma. Whereas most studies focus on the access to H-mode, the H-L back transition is less explored. This work examines the evolution and properties of JET plasmas with the ITER-like wall [2] at the H-L back transition in relation to the forward L-H transition. The influence of the wall composition (C vs Be/W), in particular on the density evolution, radiation losses and impurity composition, is also analysed, through direct comparison of forward and back transitions in JET-C and JET-ILW plasmas.

2. L-H and H-L transitions experiments. L-H and H-L transitions are studied in JET by means of slow power ramp up/down (~ 1 MW/s) experiments to enable power threshold measurements. Both the loss power, $P_{loss} = P_{heat} - dW/dt$, and the net power through the separatrix, $P_{sep} = P_{loss} - P_{rad,bulk}$, are analysed. $P_{rad,bulk}$ is the radiated power from the bulk plasma, evaluated as the total radiated power measured by bolometry integrated over the plasma volume to the 98% flux surface. Comparison of L-H transitions in JET-C and JET-ILW are reported in [3], [4]. The experiments on the H-L back transition reported here were carried out at Ip/B_T = 2.75MA/3.0T, δ= 0.35 and with the same divertor geometry (the currently installed MkII-HD divertor), both with JET-C and JET-ILW. A gradual transition from H-mode to L-mode is observed, making the identification of the transition time, t_{H-L}, difficult to pinpoint. We define t_{H-L} as the time of the loss of the edge T_e pedestal, as measured by fast ECE.

3. Power threshold and hysteresis. No or weak hysteresis is observed in the power threshold, both for P_{loss} and P_{sep}, namely $P_{L-H} \sim P_{H-L}$ for a given density (Figures 1 and 2), thus accounting for the core radiation does not explain the lack of hysteresis in power in JET. Moreover, the lack of hysteresis in the power threshold is independent of the JET wall composition (Figures 1 and 2) and consistent with earlier findings with JET-C [5]. With JET-ILW, the H-L transition occurs at higher plasma density than the L-H forward transition (Figures 1 and 2). For this reason, it is not possible to determine whether the non-monotonic dependence of P_{L-H} vs density observed at low density for the L-H transition in JET-ILW [3], [4] is also found for P_{H-L}. Conversely, with JET-C the H-L back transition occurs at similar or even lower density than the forward L-H transition, thus the two datasets overlap well in terms of density range (Figures 1 and 2). Both P_{L-H} [3], [4] and P_{H-L} are found to increase monotonically with density with JET-C and MkII-HD divertor geometry (Figures 1 and 2). Since the L-H power threshold is approximately 30% lower in JET-ILW than in JET-C in the high density branch [3], [4], also the H-L power threshold is accordingly reduced in JET with the full metal wall.

4. Plasma radiation and impurity composition. Analysis of the radiated power distribution in the plasma shows that, at a given density, JET-ILW plasmas are characterized by similar levels of edge radiation ($P_{rad,edge}$ = radiated power from divertor and X-point region) normalized to P_{loss} at the L-H and H-L transition, but higher normalized bulk radiation $P_{rad,bulk}/P_{loss}$ at the H-L back transition (by roughly a factor of two). The latter finding is due partly to an increase in high Z impurity concentration (mostly W, but also Ni) during the H-mode phase of the discharge and partly to the fact that the H-L transition occurs at higher density than the forward L-H transition. JET-C plasmas instead exhibit similar values of $P_{rad,edge}/P_{loss}$ and $P_{rad,bulk}/P_{loss}$ at the L-H and H-L transition.

The line averaged Z_{eff} is strongly reduced from JET-C to JET-ILW (Figure 3), due to i) the strong reduction in C concentration after the transition to full metal wall [6] ($c_C \sim 0.05\%$ in JET-ILW as opposed to $c_C \sim 0.5 - 1\%$ in JET-C, as measured by edge CXRS at the L-H transition [4]), ii) the reduction in Z of the main intrinsic impurity (*Be*) and iii) the absence of chemical sputtering for *Be*. Both in JET-C and in JET-ILW similar values of Z_{eff} are measured at the L-H and H-L transition (Figure 3). The lower power threshold and edge temperature observed at the L-H (and H-L) transition in JET-ILW [3], [4] may be linked to the reduction in Z_{eff} from JET-C to JET-ILW [7].

5. Edge ion profiles and radial electric field at L-H and H-L transitions. Analysis of the local parameters shows that the edge electron temperature, $T_{e,edge}$, measured at the location of the pedestal top in the H-mode phase, is similar at the L-H and H-L transition, except at very low densities, accessed only in the C-wall dataset, where $T_{e,edge}$ *(H-L)* is somewhat higher than $T_{e,edge}$ *(L-H)*, as shown in Figure 4. Furthermore, similar values of line averaged Z_{eff} and strong coupling of $T_{i,edge}$ and $T_{e,edge}$ at the forward and back transitions at a given density indicate that also the ion pressure is similar, p_i*(L-H)* ~ p_i*(H-L)*.

The leading theory for the L-H transition and the formation of the H-mode edge transport barrier is that a critical *ExB* shear is needed to suppress L-mode turbulence and trigger the transition to H-mode. We thus examine the edge radial electric field, E_r, in JET across the L-H and H-L transitions. The edge E_r is calculated from the radial force balance of C^{+6} impurity ions, as measured by the edge CXRS diagnostic: $E_r = grad(p_I)/(Ze\, n_I) - v_{pol}B_{tor} + v_{tor}B_{pol}$. The JET edge CXRS diagnostic has been significantly refurbished prior to the ILW campaign, leading to improved ion impurity profiles [4]. At the L-H transition a weak impurity ion diamagnetic term is observed (Figure 5, left) and the $v_{tor}*B_{pol}$ term does not contribute to the depth of the E_r well, but is the dominant contributor to the E_r shear more radially inwards, indicating that v_{tor} may not play a role in the formation of the edge transport barrier. Low values of impurity ion poloidal velocity are measured in JET-ILW, with no measurable evolution from L-mode to H-mode and back to L-mode, within the experimental uncertainties: $v_{pol} \leq 5$ km/s ± 2-3 km/s [4]. Such low values of v_{pol} are consistent with previous measurements of poloidal velocity from JET [8], [9], but in contrast to observations from other tokamaks, where poloidal velocities of significant magnitudes have been measured in H-mode (see e.g. [10] for recent results on ASDEX- Upgrade and references therein). In the present work v_{pol} is assumed on average equal to zero (within the experimental uncertainties) and thus the $v_{pol}*B_{tor}$ term is neglected in the calculation of E_r. Under this assumption, shallow, negative E_r wells are measured at the L-H transition, of order $E_r \sim 2 - 4$ kV/m (Figure 5, left). In parallel, the measured v_{pol} is being compared with neoclassical theory in the L-mode and H-mode phases in order to determine the total E_r profile.

Shallow E_r wells are also measured at the H-L back transition, as shown in Figure 5 (right) and Figure 6, although somewhat deeper than those observed at L-H, possibly because the back transition occurs at higher density than the forward L-H transition. Whereas at the L-H transition the ion impurity diamagnetic term of the E_r well is driven mainly by the $T_i/Z*$ $grad(n_I)/n_I$ component, at the H-L back transition both $T_i/Z*$ $grad(n_I)/n_I$ and $grad(T_i)/Z$

components contribute with similar strength to the depth of the E_r well.

The evolution of E_r across the L-H transition, into the H-mode phase and across the H-L transition is shown in Figure 5 (right) for the JET-ILW discharge at highest density in the dataset (see e.g. Figures 1 and 2). The shallow and broad E_r well observed at the L-H transition doubles in strength 10 ms after the transition (corresponding to the next edge CXRS frame). In the developed H-mode phase (pre ELM phase) the E_r well is deeper and narrower, has moved radially inwards and is mainly driven by the steep gradient of the T_i profile. At the H-L back transition the E_r well has reverted to a broader and shallower shape, while still being located radially inwards and being somewhat deeper than the profile at the L-H transition. In general, similar E_r values are found at the forward and back transition, as shown in Figure 6. This result is consistent with the global measurements indicating similar power thresholds at the forward and back transition and would support the theory of a critical *ExB* shear suppressing turbulence at the L-H transition.

6. Conclusions. Analysis of slow L-H and H-L transitions in JET generally indicates a lack of hysteresis in the power threshold, both in JET-C and in JET-ILW. On the basis of this evidence, ITER scenarios that rely on hysteresis of the L-H power threshold to achieve the reference operating conditions should be revisited. The edge radial electric field, measured from the radial force balance of C^{+6} impurity ions, is of similar magnitude at the L-H and H-L transition, under the assumption of a negligible v_{pol}*B_{tor} term as indicated by the edge CXRS measurements. This result - if confirmed by comparison of the measured vpol with the neoclassical value - together with the observation that $P_{L\text{-}H} \sim P_{H\text{-}L}$, would support the theory of a critical *EXB* shear needed to suppress L-mode turbulence and trigger the H-mode.

References:

[1] C. Kessel, ITPA-IOS Meeting, April 2012. [2] F. Romanelli, "Overview of the JET results with the ITER-like wall", 24th Fusion Energy Conf., 2012, San Diego. [3] C.F. Maggi et al., Proc. 39th EPS Conference, Stockholm, 2012, O3-108. [4] C.F. Maggi et al., to be submitted to Nucl. Fusion.

[5] Y. Andrew et al., Plasma Phys. Control. Fusion **50** (2008) 124053. [6] S. Brezinsek et al., JNM **438** (2013) S303. [7] C. Bourdelle et al., this Conference. [8] N. Hawkes et al., Plasma Phys. Control. Fusion **38** (1996) 1261. [9] Y. Andrew et al., EPL **83** (2008) 15003. [10] E. Viezzer et al., Nucl. Fusion **53** (2013) 053005.

This work was supported by EURATOM and carried within the framework of EFDA. The views and opinions expressed herein do not necessarily reflect those of the European Commission.

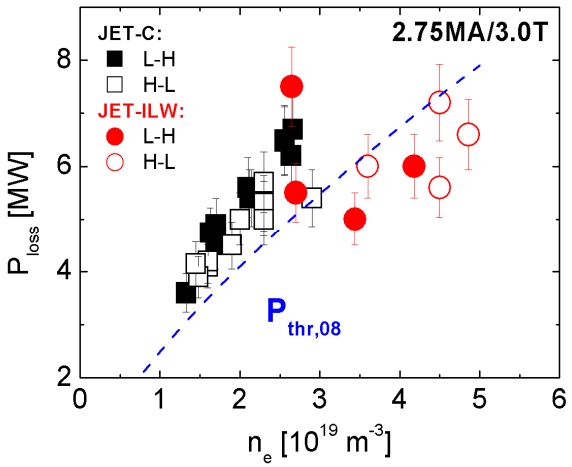

Figure 1. Loss power vs central line averaged density at L-H and H-L transitions for JET-C and JET-ILW. The L-H threshold ITPA scaling law $P_{thr,08}$ is noted by the dashed blue line.

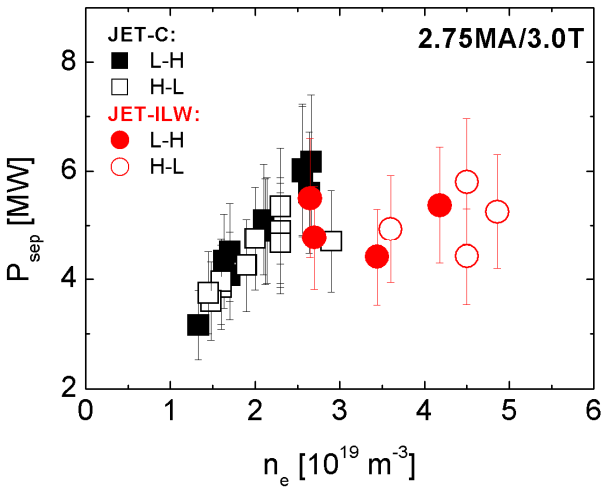

Figure 2. Net power across the separatrix ($P_{sep} = P_{loss} - P_{rad,bulk}$) vs central line averaged density at L-H and H-L transitions for JET-C and JET-ILW.

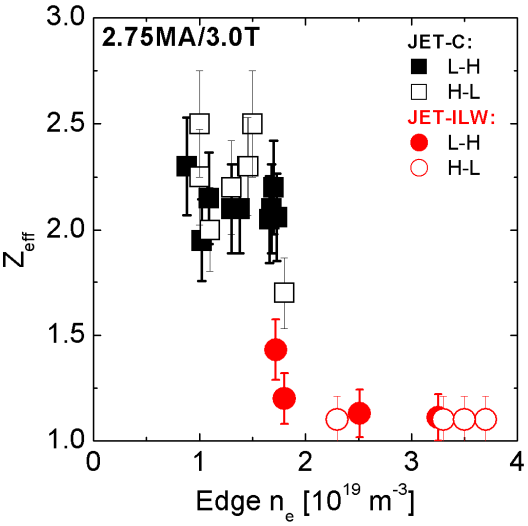

Figure 3. Line averaged Z_{eff} at L-H and H-L in JET-C and JET-ILW discharges.

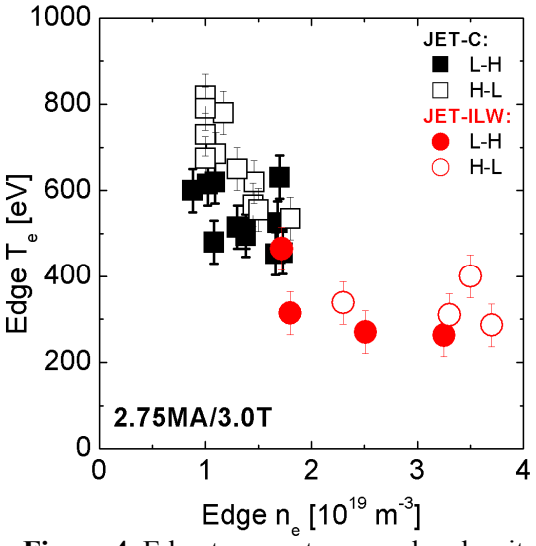

Figure 4. Edge temperature vs edge density (at the location of the pedestal top in the H-mode phase).

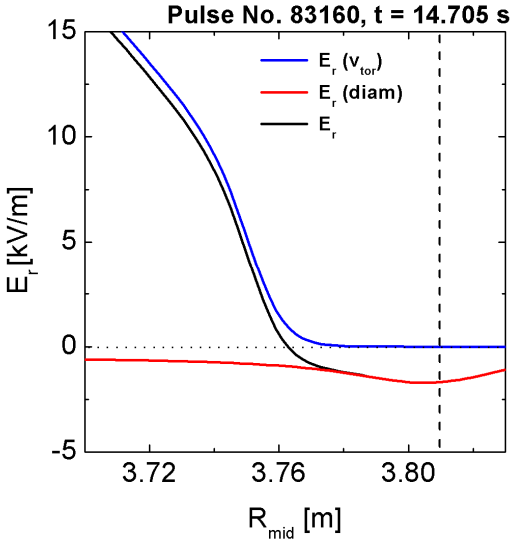

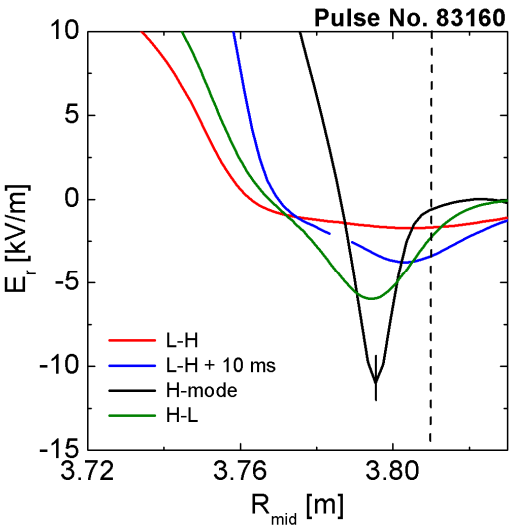

Figure 5. Left: Edge radial electric field at L-H transition (JET-ILW, higher density shot of Figure 1 and 2) and right: Evolution of E_r from L-H to H-mode phase and H-L phase (H-L – 30 ms). The vertical dashed line corresponds to the separatrix position.

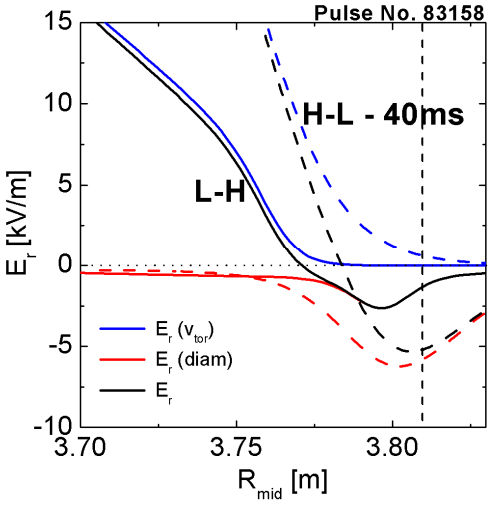

Figure 6. Edge radial electric field at L-H and 40 ms prior to H-L transition. The vertical dashed line corresponds to the separatrix position.